RESEARCH ARTICLE **OPEN ACCESS**

SYNTHESIS OF FATTY ALCOHOLS BY HYDROGENATION OF PALM ESTERS USING RHENIUM-BASED CATALYSTS SUPPORTED ON NIOBIA, ALUMINA AND TITANIA

Germildo J. Muchave[1], Leonardo D. de S. Netto[2], João M.A.R. Almeida[3] and Donato A. G. Aranda[1]

[1]EPQB, Escola de Química, Universidade Federal do Rio de Janeiro, Av. Athos da Silveira Ramos, 149, RJ, 21941-909, Brazil; [2]Programa de Engenharia Química, COPPE, Universidade Federal do Rio de Janeiro, Av. Athos da Silveira Ramos, 149, RJ, 21941-972, Brazil; [3]Instituto de Química, Universidade Federal do Rio de Janeiro, Av. Athos da Silveira Ramos, 149, RJ, 21044-020, Brazil

ARTICLE INFO

ABSTRACT

Hydrogenolysis of esters to fatty alcohols (FA) investigated using Re catalysts with different supports. First, the catalysts were prepared through incipient wetness impregnation and characterized. The catalysts were tested at different temperatures and pressure. The catalysts supported on Al_2O_3, Nb_2O_5 showed faster conversion rates. However, the selectivity to FA decreases during the reaction favoring hydrocarbons (HC) production, especially at higher temperatures. The Re/TiO_2 catalyst obtained a higher selectivity of 93.8% in FA and a conversion of 92% at 280 ºC. The Re/Nb_2O_5 catalyst obtained excellent yield with 99.7% conversion and 86.7% selectivity in AF at a temperature of 250 ºC and 70 bar.

INTRODUCTION

The development of new technologies devoted to biomass conversion into high added-value products or renewable energy has been a challenge in recent years. Among these applications, the synthesis of fatty alcohols stands out through esters or fatty acids hydrogenolysis using catalysts under certain specific conditions. The use of vegetable oils or their derivatives (esters or fatty acids) in the industry as a natural input for obtaining several products with high added value has been shown to be a reality today. The conventional process of producing copper-based fatty alcohols and using chromium from an environmental and energy efficiency point of view is not feasible; operational conditions of severe temperature and pressure, 250-300 ºC, and 2000-3000 psi are applied, respectively (Thakur and Kundu 2016) [Thakur, 2016 #1]. For these reasons, in recent years, both mild operating conditions and other types of catalysts have been developed for converting triglycerides and their derivatives into fatty alcohols or other bioproducts, in particular hydrocarbons (Miyake, Makino et al. 2009). Some of the catalysts and mild conditions that have stood out in new processes are, for

example, Rh-Sn-B (Benítez *et al.* 2019); Ni/ZrO_2 (Ni *et al.* 2019); Cu-Fe (Hattori *et al.* 2000); Cu-Zn (Huang *et al.* 2009) and $ReOx/TiO_2$ (Rozmysłowicz, et al. 2015). The application of noble metal catalysts would be useful because they generally have more excellent hydrogenation reactions. However, it is necessary to control the operational conditions to avoid the transformation of fatty alcohol (product of interest) into hydrocarbons (Carnahan *et al.* 1955, Cui *et al.* 2015, Rozmysłowicz *et al.* 2015). In addition to the different metals tested in the formulation of catalysts, several supports are also being tested, such as ZrO_2, SiO_2 (Ali *et al.* 2019), TiO_2 (Rozmysłowicz *et al.* 2015, Ali *et al.* 2019), Al_2O_3 (Huang, et al. 2009, Miyake *et al.* 2009, Ali *et al.* 2019). A number of studies have recently shown that niobium is a reducible oxide that has been widely applied successfully in several processes (Masuda *et al.* 1985, Zhao *et al.* 2012, Zhou *et al.* 2013, Shao *et al.* 2017). These various niobium oxide applications were crucial in choosing niobium oxide to support the production of fatty alcohols in the present study based on rhenium. In some studies, rhenium has shown promising activity in hydrogenation reactions and selectivity in fatty alcohols

(Mendes *et al.* 2001, Manyar *et al.* 2010, Rozmysłowicz *et al.* 2015). The research also aims to compare rhenium catalysts catalytic activity supported on different supports (Al2O3, Nb2O5, and TiO2). The hydrogenation of fatty acid esters of fatty acids to obtain fatty alcohols can be carried out in a multiphase system (van den Hark and Härröd 2001, Zhilong 2011), which is characterized by low hydrogen solubility in the substrate and high resistance to the transport of pasta. Alternatively, in a homogeneous system with the aid of solvent to overcome these limitations of the multiphase system (Manyar *et al.* 2010, Rozmysłowicz, et al. 2015). In this work, heptane was used as an organic solvent in the reactions. According to Manyar *et al.* (2010), Zhilong (2011) organic solvents help control the concentration of hydrogen on the catalyst surface without depending on the other factors involved, thus reducing the heterogeneity between the reactants and the catalyst under mild conditions of temperature and pressure.

MATERIALS AND METHODS

Reagents and Equipment: The reagents used in this work were palm ester (Agropalma S.A.), Perrenic Acid (HReO$_4$, Sigma-Aldrich), Hydrogen 99.99 % (Linde Gases) gamma-alumina (γ-Al$_2$O$_3$, SASOL), Aeroxide TiO$_2$ P90 (Degussa) and niobium oxide (Nb$_2$O$_5$, CBMM). The experiments were carried out in a Parr reactor of 300 mL volume, model 4848 with stainless steel beaker, automatic temperature, and pressure control. The equipment has a gas supply system and is equipped with a stirring and speed regulation shaft.

Catalysts preparation: The addition of rhenium was carried out through incipient wetness impregnation. In this case, the amount of water used to dilute perrenic acid for each support varied based on pores volume. It was determined according to the pore volume obtained in Nitrogen Physisorption analysis for each support. After the rhenium salt was impregnated in supports, catalysts were placed oven for 12 h at a temperature of 100 ^{o}C. Then they were calcined at 500 °C, for four (4h), with a heating rate of 5 °C/min, except for the catalysts supported on Nb$_2$O$_5$, which, calcined at 400 ^{o}C.

Characterization of catalysts: The determination of the catalysts textural properties and supports in terms of specific surface area, pore-volume, and average pore diameter were obtained through adsorption isotherms and nitrogen desorption at -196 ^{o}C in a TriStar II 3020 V1.03 equipment. Initially, 0.3 g of catalyst or support weighed as appropriate. The samples were pre-treated at 300 °C for 12 h under vacuum to remove water and compounds possibly adsorbed on the samples surface. Finally, the materials textural properties were determined: the superficial area (BET method) and the pore volume. Analyses by temperature-programmed reduction of the catalysts were carried out in Micromeritics Autochem TPR-2920 Crycooler II model equipment. First, about 30 mg of the catalyst sample was weighed, then the samples were inserted in a quartz reactor coupled to a unit equipped with a temperature-controlled oven, thermal conductivity detector (TCD), micrometric valves for controlling the gas flow rates of both H$_2$/Ar and nitrogen reducer and pretreatment, respectively. The gas flow was 50 mL/min. First, the sample was pre-treated at 150 ^{o}C for 30 min. Then it was cooled to room temperature (between 25-30 ^{o}C), then reduced at a rate of 10 ^{o}C/min to 1000 ^{o}C. The reduction data were collected on a computer coupled to the equipment in real-time analysis. The

X-ray diffraction analyses were performed to study the crystallinity of the catalysts and supports. For the analysis, a certain amount of the sample was placed in a small specific glass plate.

A Rigaku transmission diffractometer, Miniflex II, with a monochromator and Cu tube was used, under an angular scan that varied between 5 to 90º, the increment of 0.05, counting time of 1 s/step and without a knife. The analyzes TPD of the ammonia were carried out in a mass spectrometer QMS-200 (Balzers), with the ratio m/z = 15, used to quantify the ammonia. Adsorption of ammonia was carried out at a temperature of 70 °C using a mixture of 4 % NH$_3$/He with a flow rate of 30 mL/min for 30 min; after this period, a purge with pure He performed for 60 min. The desorption of the chemisorbed ammonia was carried out by heating the samples to 800 °C at 20 °C/min. Quantification of the desorbed ammonia from the catalysts was performed by integrating the area under the intensity versus time curve.

The analyses performed using an X-ray photoelectron spectroscopy (XPS) model ESCALAB 250Xi. The equipment is coupled to the XPS spectrometer with high sensitivity with high-resolution quantitative images and equipped with multi-techniques to analyze the electronic characteristics and chemical composition of the surfaces. The infrared spectroscopy with Fourier transformation (IFTR) of pyridine technique was applied to determine the Lewis and Bronsted acid sites in the catalysts. For this, the Shimadzu IRPrestige-21 equipment was used. 0.1 g of catalyst was weighed in a flask, and then 1 ml of pyridine in the liquid phase was added and manually stirred. Then the flask was placed in the oven at 100 °C to evaporate the pyridine. After drying, the sample was analyzed with IFTR in the range of 1400-1580 cm^{-1}, with a resolution of 2 cm^{-1} and one (1) sweep. The background was made with the samples calcined without adsorption of pyridine (Menezes *et al.* 2020).

Kinetic of hydrogenation reactions: The kinetic study of the catalysts was carried out under temperature conditions ranging between 250 and 280 ^{o}C, and the pressure was set at the 70 and 40 bar. Heptane was used as a solvent in all reactions in the ratio in relation 1:3 to the fatty acid ester (ester: heptane). Sampling was performed in the following reaction times: 5, 10, 30 min, 1, 2, 3, 4, 5, 6, 7, and 8 h to construct the kinetic curve. The reactions were carried out at constant hydrogen pressure of 70 or 40 bar. The supply of hydrogen in the reactor was a semi-batch operation. Hydrogen pressure was added to the reactor for maintaining the reaction pressure, whereas hydrogen is consumed or in each aliquot that was removed. The chemical reactions in the hydrogenation of these fatty acid esters can vary depending on the reaction conditions.

RESULTS AND DISCUSSION

Characterization of the catalysts

Textural properties: Table 2 shows the textural properties (surface areas and BJH pore volume) of supports and catalysts. Based on those in Table 2, the change in textural properties (surface area and pore volume) was evident about their respective supports' textural properties. The surface areas and the pore volume decreased. This modification of the porous structure and the substrates surface area may be related to some factors, such as sintering during calcinations (Schäfer et al. 1966, Viet *et al.* 2010, Massa *et al.* 2013). The second

factor linked to the slight modifications in reducing pore volume and pore size is phase alter of the samples and the sintering between the crystallites. On the other hand, it can be caused by the superficial diffusion mechanism. The synthesized monometallic catalysts suffered a decrease in their surface areas and porous structure compared to their respective supports structural properties. However, surface areas of Re/Nb_2O_5 and Re/TiO_2 suffered a sharp decline compared to those of Nb_2O_5 and TiO_2. Similar results were obtained by Paulis *et al.* (1999), where they demonstrate that the increase in the calcination temperature reduced the surface area, both of the catalysts and the supports.

**Table 2. Textural properties of supports and catalysts**

Catalysts	Surface area -BET (cm²/g)	Pore volume (cm³/g)
Al_2O_3	161	0.38
Nb_2O_5	207	0.31
TiO_2	103	0.17
Re/Al_2O_3	140	0.39
Re/TiO_2	43	0.17
Re/Nb_2O_5	79	0.13

X-Ray Diffraction: Figure 1 shows the results of the supports crystallinity. While in Figure 2 illustrates the results of the catalysts the crystallinity. Figure 1 illustrates that the alumina support $(\gamma\text{-}Al_2O_3)$ has an amorphous structure, with three peaks of the X-ray diffractogram found at 37.5, 45.8, and 67.0^o. These peaks are characteristic of $\gamma\text{-}Al_2O_3$; this result is in accordance with the literature (Augustine and Sachtler 1989, Miyake *et al.* 2009). Niobium oxide (Nb_2O_5) also had an amorphous structure that peaked at 26.5 and 53.6^o. Griffith *et al.* (2016), in their work calcined Nb_2O_5 at 600 ^{o}C, found a diffractogram of a crystalline structure.
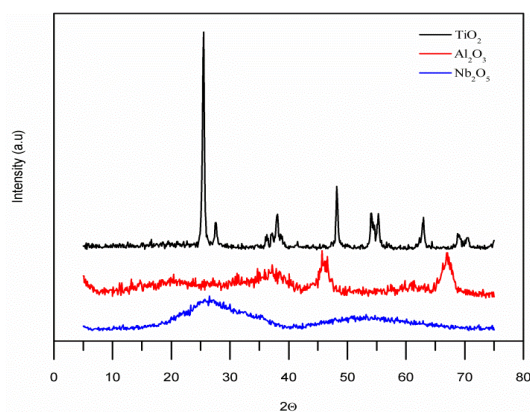
Figure 1: X-ray diffractogram of the supports

These authors characterized this crystalline structure of T-Nb_2O_5 as topology in the form of crack that oxide suffers from increased temperature. Titanium oxide (TiO_2) has a crystalline structure with several peaks. Its characteristic peaks $2\theta = 25.5$, 37.9, 48.1, 54.6, 62.8, 70.0, and 75.2^o. According to Ohama and Van Gemert (2011), TiO_2 change its crystalline structure depending on the phase in which it was obtained. This result contributes to TiO_2 to be applied in several areas due to its crystallographic properties. Figure 2 shows the diffractograms of monometallic catalysts, where these present only peaks that correspond to the supports used in Figure 3; that is, it was not possible to detect the peaks that correspond to rhenium. Similar results were observed for Re/TiO_2 catalyst (Di *et al.* 2019, Ting *et al.* 2019) and Re/Al_2O_3 catalyst (Ma *et al.* 2018).
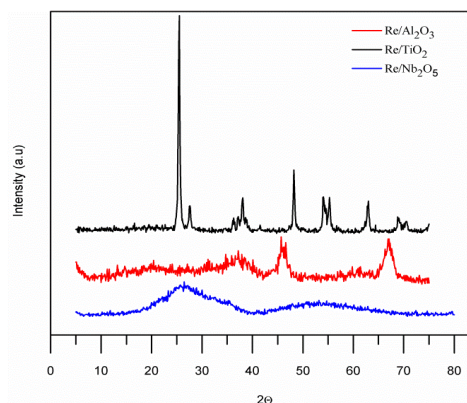

Figure 2. X-ray diffractogram of catalysts

The absence of rhenium peaks in the diffractogram maybe because the rhenium content is minimal or that was more excellent dispersion of the metal on the surface of the supports (Di *et al.* 2019). According to Di *et al.* (2019), the peaks of the Re/TiO_2 catalyst are attributed to the support phases of TiO_2 (anatase and rutile). The other aspect is that the catalysts supported on Al_2O_3, and Nb_2O_5, showed no difference in their crystallinity from their peaks, having shown amorphous structures. As for the catalysts prepared in TiO_2, there was not much difference in the crystallinity peaks in calcined and non-calcined supports. The main difference found is the difference in peak intensity between the catalysts. This difference in peaks is related to the difference in the calcination temperature.

Temperature Programmed Desorption of Ammonia: The total acidity profiles of TPD-NH_3 of the catalysts are shown in Figure 3 and Table 3.

Table 1: Amount of NH3 desorbed

| Catalyst	NH_3 ($\mu mol_{NH3}/g_{cat}$)	Ratio acid site (%)	
		Weak	Strong
Re/Nb_2O_5	499.1	43.3	56.7
Re/TiO_2	203.3	36.4	63.6
Re/Al_2O_3	575.9	12.0	88.0

The deconvolution areas values and the temperature ranges in which the ammonia desorption occurred are shown in the table. TPD-NH_3 results showed similar profile of the adsorption graphs for catalysts Re/TiO_2, and Re/Nb_2O_5, except the catalyst Re/Al_2O_3, which has greater width.
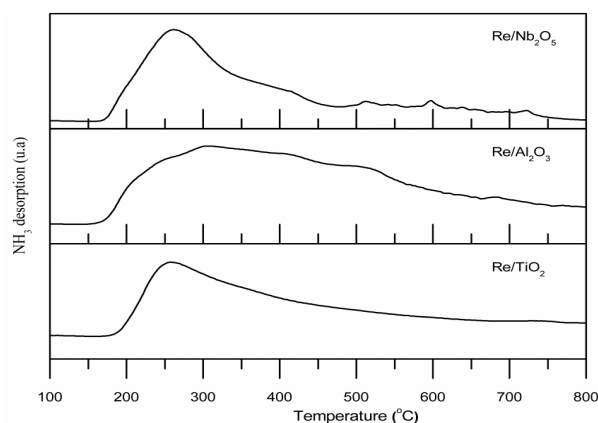
Figure 3. TPD-NH3 acidity profiles of catalysts at different

One of the main differences is related to the amount of dissolved ammonia and the desorption temperature, as shown in Figure 3 and Table 3. Table 3 shows that the catalysts acid strength increases in the order $Re/Al_2O_3 > Re/TiO_2 > Re/Nb_2O_5$. Therefore, the catalyst supported on alumina had a more significant amount of adsorbed ammonia. Similar results were found in the literature that shows the NH_3 desorption profile for Re/TiO_2 and Re/Al_2O_3 catalysts (Kirilin 2013, Ma, et al. 2018, Zhou *et al.* 2020). TPD-NH_3 results of catalysts supported on alumina show a higher amount of dissolved NH_3 than in catalysts supported on titania and niobia, corroborating the Kirilin (2013).

According to Ma *et al.* (2018), the ammonia desorption temperature in Re/Al_2O_3 catalyst peaked at 170 °C, which increased to 225 °C, indicating that the presence of Re increased the acid resistance of the Al_2O_3 support. In a comparative analysis of acidity and basicity of the Re/TiO_2 and Pt/TiO_2 catalysts, it was observed that the addition of any metal on TiO_2 always increases the acidity of the catalyst, even if not significantly. However, ammonia adsorption is always greater for the Pt/TiO_2 catalyst than in the Re/TiO_2 catalyst (Rozmysłowicz *et al.* 2015).
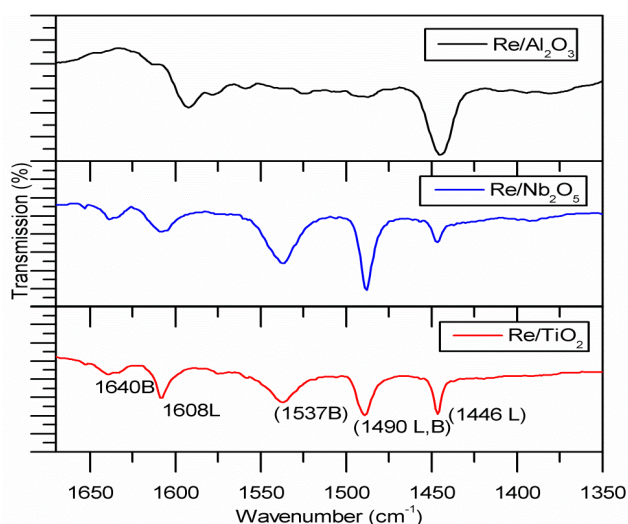
Figure 4. Comparison of spectra of catalysts produced from IFTR transmission (pyridine: (a) Re/Al₂O₃; (b) Re/Nb₂O₅; and (c) Re/TiO₂

Infrared Spectroscopy with Fourier Transformation: Figure 4 shows the results of the IFTR of pyridine of the qualitative nature of the acidic sites present in each of the three catalysts. According to the profile of the graphs in Figure 4, there are bands at 1445, 1490, 1609, 1537, and 1640 cm^{-1} for all catalysts.

According to Leal *et al.* (2019), da SQ Menezes *et al.* (2020), bands corresponding to Bronsted acidic sites are found at 1445, 1609 cm^{-1}, while bands referring to Lewis acidic sites are found at 1537 and 1640 cm^{-1}. As for the band at 1490 cm^{-1}, it refers to both Lewis and Bronsted sites.

The distribution of acidic sites, the Re/Al_2O_3 catalyst, showed only Lewis acidic sites, coinciding with Ma *et al.* (2018), which means that the greatest acidic force was observed in the ammonia desorption in the TPD results corresponded to the Lewis sites. Ma *et al.* (2018) found that results through IFTR that γ-Al_2O_3 is characterized mainly by Lewis acidic sites. On the other hand, the IFTR and CO_2-TPD showed that the

impregnation of rhenium in alumina does not affect the type of acidic sites and has little impact on the base character of the catalyst, respectively (Ma *et al.* 2018).

As for the Re/Nb_2O_5 catalyst, it presented both Lewis and Bronsted acid sites. However, it was evident through the bands' intensity that has more Bronsted acid sites than Lewis. According to the literature, catalysts supported on Nb_2O_5 have both Lewis and Bronsted acids. Bronsted's acidic sites availability in rhenium-containing catalysts increases with the increase in rhenium content in the catalyst; however, Lewis's acidic sites do generally not vary (Zhang *et al.* 2012). According to Chia *et al.* (2013), the NH_3 TPD results used to quantify the acidic sites showed the presence of Brønsted acidic sites of the RhRe/C catalyst. The authors believe that these acidic sites' formation may have been due to the deprotonation of hydroxyl groups in rhenium atoms associated with rhodium.

However, for nickel catalysts supported on niobia, the availability of these acidic sites in the catalysts may vary with the content of the supported metal; that is, Brønsted acidity decreases as the Ni charge has been increased, but Lewis acidity seems to be preserved mainly even with such a high Ni load on Nb_2O_5 (Leal *et al.* 2019). The Re/TiO_2 catalyst profile also showed Bronsted and Lewis acidic sites. However, in this case, there seems to be a balance of acidic forces; that is, there does not seem to be one type of acidic site that is larger than the other. The literature has shown IFTR analyzes for pyridine adsorbed in both Re/TiO_2 and TiO_2 have a higher amount of Lewis acid sites and some traces of Bronsted acid sites (Augustine and Sachtler 1989, Malinowski *et al.* 1998).

X-Ray Photoelectron Spectrometer: Figure 5 illustrates the XPS graphics profile of the Rhenium (Re) catalysts on the different supports. The fitting of the spectra curves revealed a doublet for all catalysts with a more intense Re 4f7/2 reference peak and the second Re 4f5/2 peak. Figure 5 shows the adjustment curves of the XPS spectra of the three (3) rhenium catalysts. Based on the profile of the graphs, it can be seen that the rhenium has a doublet. The doublet corresponds to Re 4f7/2 and Re 4f5/2, which indicates a single Re species' presence. Similar observations have already been reported in the literature (Escalona *et al.* 2007). The binding energies of the catalysts and the respective atomic ratios of the rhenium on the supports are shown in Table 4.

Table 4 confirms the results shown in Figure 5 that in all catalysts, a single species of rhenium was observed in the catalysts, which is Re^{7+}. On the other hand, in Table 4, the spectrum of the binding energies for the Re/Nb_2O_5, Re/TiO_2, and Re/Al_2O_3 catalysts are not very wide. This may indicate that there are only Re^{7+} species present on the surface of the catalysts that are in a homogeneous dispersion on the surface of the supports.

The use of different supports did not influence the variation of rhenium species that are present in the catalysts. Probably because it is the same rhenium charge in the three catalysts. Although some have found similar results, in which only a single species of rhenium Re^{+7} was found, in the literature, there are works in which they found more than one species of rhenium in the catalysts (Ly *et al.* 2015, Toyao *et al.* 2017). According to Ly *et al.* 2015), the variation in the content of rhenium in the catalysts can lead to a tendency to distribute the species of this metal in the catalyst.
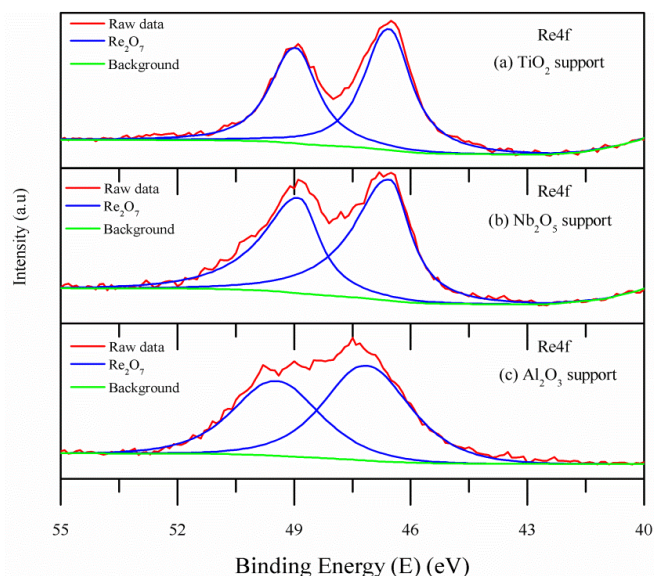
Figure 4. Rhenium XPS spectra in monometallic catalysts: (a) Re/TiO₂, (b) Re/Nb₂O₅ and (c) Re/Al₂O₃

That is, that the Rhenium species, depending on the load, change to more oxidized species as their content in the catalyst increases. The XPS results of the Re/TiO₂ catalyst showed that the catalyst had two species of rhenium Re4f7/2 and Re4f5/2 with atomic concentrations of 56 and 44 %, respectively (Malinowski *et al.* 1998). After the reduction, the authors found that the catalysts may present species with less oxidized Re oxidation, such as Re^{+3} and Re^{+4} (Isaacs and Petersen 1982, Toyao *et al.* 2017). Results show metallic dispersion of rhenium on the supports (Nb₂O₅, Al₂O₃, and TiO₂), based on the atomic ratio that the dispersion increases in the following order: Re/Nb₂O₅ > Re/TiO₂ > Re/Al₂O₃. According to the result of XPS with loading completely oxidized samples, the greater the atomic ratio of one metal to another or the support suggests the presence of well-dispersed surface species of the metal (Kerkhof and Moulijn 1979). Therefore, the Re/Nb₂O₅ catalyst with an atomic ratio of Re/Nb is 3.1 showed excellent dispersion. The literature indicates two reasons that may be determinant for the metallic dispersion of rhenium on the supports surface: the calcination temperature determines one reason. According to Okal *et al.* (2004), when studying the Re/γ-Al₂O₃ catalyst, they observed that the Re/Al rhenium metallic dispersion increased with increasing temperature. The increase in temperature also favors the formation of Re^{7+} species. The metal charge is also a determining factor in its dispersion on the surface of the support. According to the Yide *et al.* (1986), Bare *et al.* (2011), Re/Al₂O₃ catalyst, observed that the smaller the amount of the metal (Re) in the impregnated in the catalyst, the greater the dispersion of this metal on the support surface. The Re/Nb₂O₅ catalyst, calcined at a temperature of 400 °C, lower calcination temperature than the Re/TiO₂ and Re/Al₂O₃ catalysts, showed more excellent metallic dispersion. This dispersion may have been because Nb₂O₅ is a reducible oxide. This would justify that the two reducible oxides (Re/Nb and Re/Ti) had more excellent metallic dispersion than Re/Al.

According to Massa *et al.* (2013), the catalysts supported on TiO₂ usually show greater metals dispersion on the support surface. These authors believe that the excellent dispersion of metals on the TiO₂ surface can be obtained because titania appears to be highly dehydroxylated after metal oxide deposition. However, Rozmysłowicz *et al.* (2015) believes

that the greatest dispersion is because it is a reducible metal. Reducible transition metal oxides represent an attractive alternative to other catalytic systems. Its reactivity is essentially linked to the partial reduction of surface metal oxide species under reaction conditions (Ghampson *et al.* 2016).

Temperature Programmed Reduction (TPR): Figure 6 shows the following peaks of reduction temperatures for the catalysts: Re/Al₂O₃ catalyst (375.5 and 393.6 °C); Re/TiO₂ catalyst (251.2 °C) and Re/Nb₂O₅ catalyst (398.2 °C). Some studies corroborate the reduction profile of the Re/TiO₂ catalyst (Azzam *et al.* 2007, Di *et al.* 2019, Zhou *et al.* 2020) and Re/Al₂O₃ (Okal *et al.* 2004, Okal 2005, Bare *et al.* 2011, Thompson and Lamb 2016). In all the catalysts, there was a reduction of a single species of rhenium; that is, the peaks obtained were attributed to reducing the species from Re^{+7} to Re^0 without necessarily having passed through the intermediate species (Re^{+6}, Re^{+5}, and Re^{+4}), as noted earlier in the XPS results. The reduction of partially dispersed and oxidized Re species is more complicated than the direct reduction of Re^{7+} to Re^0 (Ly *et al.* 2015). Kirilin (2013) (Kirilin 2013) obtained a peak reduction of the Re/TiO₂ catalyst at 250 °C, which was the same temperature as found in our work. However, Burch et al. (2011) (Burch *et al.* 2011) obtained two (2) reduction peaks at elevated temperature, 315 and 380 °C. The authors justify that a reduction in elevated temperature may have been due to a reduction in ReOx (Azzam *et al.* 2007, Burch *et al.* 2011) or a reduction in bulk titanium support (Burch *et al.* 2011, Kirilin 2013).
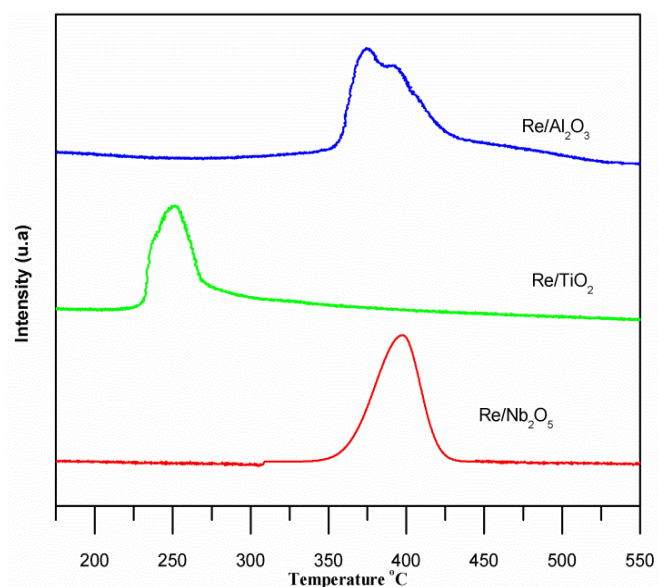
Figure 5: TPR of different Re catalysts

Even for the Re/Al₂O₃ catalyst that showed two peaks, both were attributed to the same species. The second peak at 393.6 °C in temperature corresponded to the same species with a strong connection with the support. Similar studies that showed two peaks in the reduction of rhenium catalysts were found (Bare *et al.* 2011). However, also, some studies showed a single peak reduction (Hilmen *et al.* 1996). However, all of these studies indicate that only Re^{7+} species were identified in these catalysts.

Re/γ-Al₂O₃ catalysts pre-treated at a temperature of 500 °C present species of rhenium oxide firmly attached to the alumina support (Okal *et al.* 2004, Okal 2005).
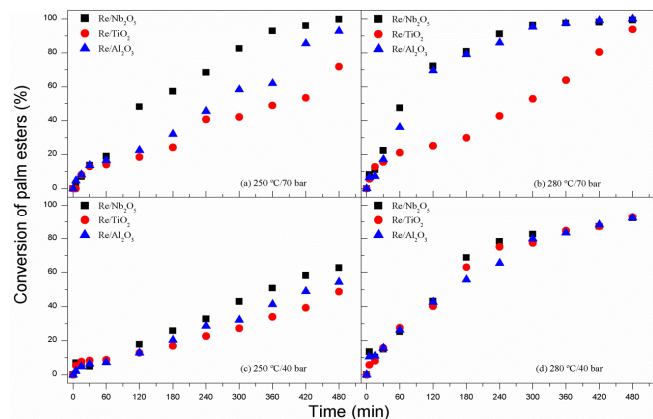
Figure 6. Conversion of palm esters: a) reactions carried out at 250 ºC-70 bar; b) reactions carried out at 280 ºC-70 bar; c) reactions carried out at 250 ºC-40 bar; d) reactions carried out at 280 ºC-40 bar

the strength of the interaction of Re in relation to the support decrease in the order $Al_2O_3 > SiO_2 > ZrO_2 > TiO_2$ (Okal *et al.* 2004, Bare *et al.* 2011, Ly *et al.* 2015, Thompson and Lamb 2016).
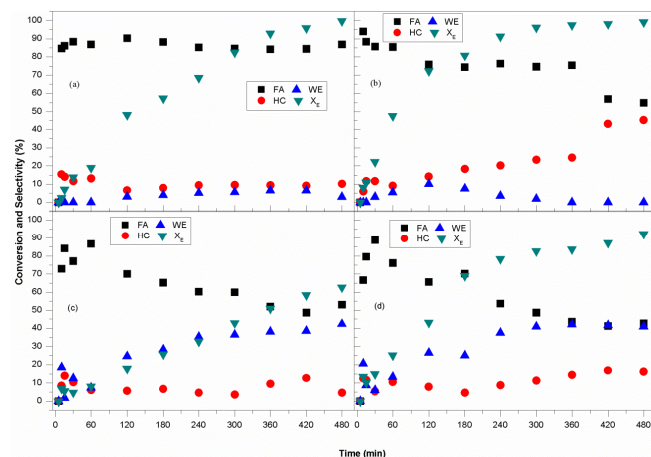
Figure 9. Conversion of esters and product selectivity (FA = fatty alcohols, HC = hydrocarbons, WE = wax esters, and XE = Conversion of products) using Re/Nb2O5 catalyst: (a) at 250 ºC-70 bar; (b) at 280 ºC-70 bar; (c) at 250 ºC-40 bar; (d) at 280 ºC-40 bar

Figure 7: Distribution profile of the products (FA = Fatty Alcohol, and HC = Hydrocarbons) obtained using the three (3) catalysts: a) reactions carried out at 280 ºC-70 bar; b) reactions carried out at 280 ºC-70 bar; c) reactions carried out at 280 ºC-40 bar; d) reactions carried out at 280 ºC-40 bar.
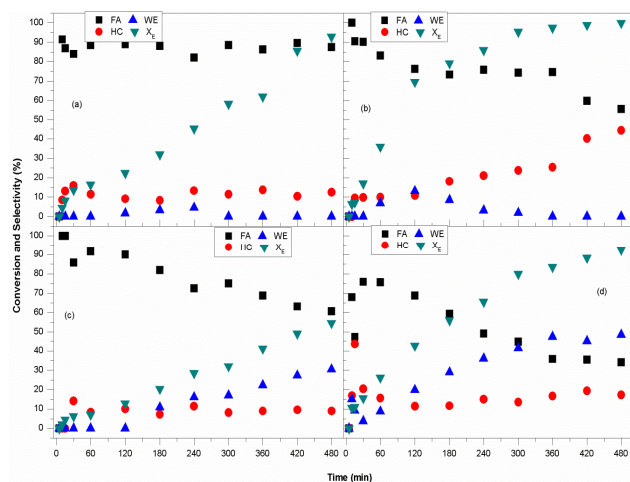
Figure 10: Conversion of esters and product selectivity (FA = fatty alcohols, HC = hydrocarbons, WE = wax esters, and XE = Conversion of products) using Re/Al2O3 catalyst: a) at 250 ºC-70 bar; b) at 280 ºC-70 bar; c) at 250 ºC-40 bar; d) at 280 ºC-40 bar
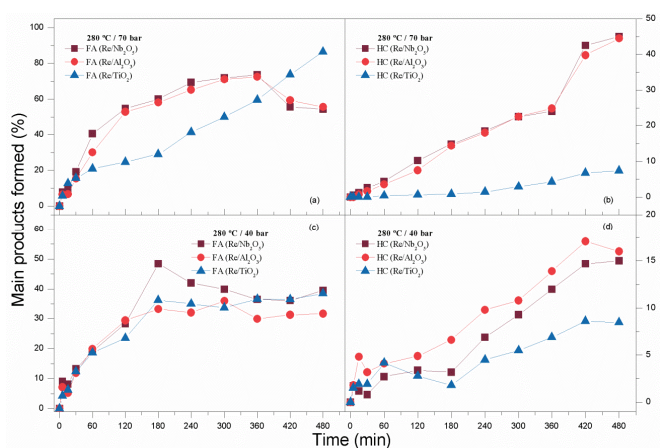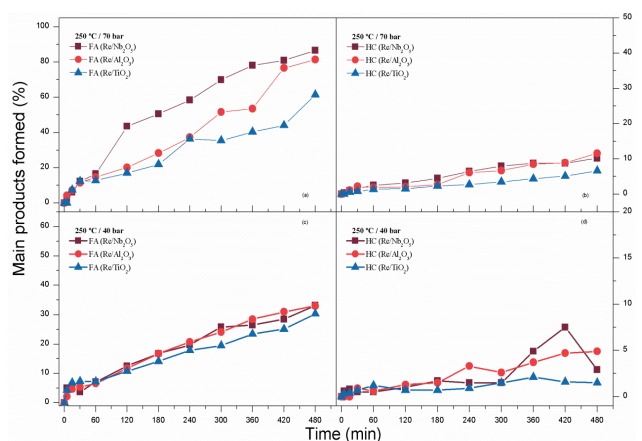

Figure 8: Distribution profile of the products (FA = Fatty Alcohol, and HC = Hydrocarbons) obtained using the three (3) catalysts: a) reactions carried out at 250 ºC-70 bar; b) reactions carried out at 250 ºC-70 bar; c) reactions carried out at 250 ºC-40 bar; d) reactions carried out at 250 ºC-40 bar
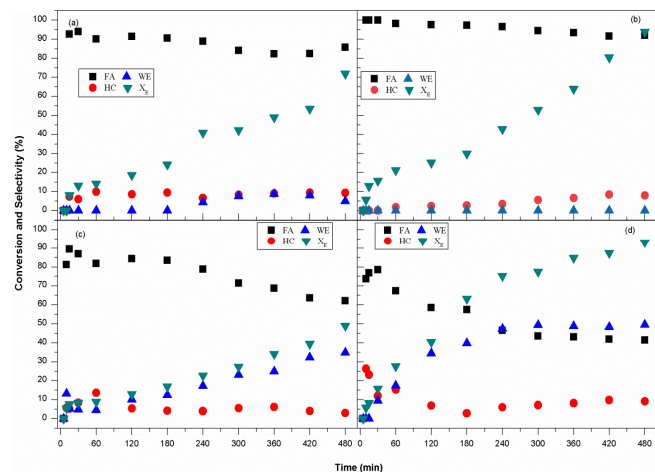
Figure 11: Conversion of esters and product selectivity (FA = fatty alcohols, HC = hydrocarbons, WE = wax esters, and XE = Conversion of products) using Re/TiO2 catalyst: a) at 250 ºC-70 bar; b) at 280 ºC-70 bar; c) at 250 ºC-70 bar; d) at 280 ºC-70 bar

The reducibility of the metal for rhenium catalysts may depend on the metal's content in the catalyst. The interaction can be very strong at low concentration and decrease with increasing coverage of Re in the catalyst (Ly *et al.* 2015). On the other hand, the calcination temperature, the adsorbed humidity, and

Table 2. Summary of the binding energies of the components of rhenium and niobium, their relative properties, and their atomic relationship of the surface between Re and the supports

Catalysts	Peaks BE (Re4f7)	FWHM eV (Re4f)	Oxidation states of Re^{7+} ions (%)	The atomic ratio (Re4f)
Re/Nb_2O_5	46.58	4.914	100.0	3.11
Re/TiO_2	46.55	4.853	100.0	2.69
Re/Al_2O_3	47.19	4.944	100.0	0.93

Therefore, this result explains and corroborates that the Re/Al_2O_3 catalyst has been reduced to a higher temperature than the Re/TiO_2 catalyst.

Kinetic of Palm Esters Hydrogenation: The experimental data show that the process of converting unsaturated esters (methyl linoleate and methyl oleate) into saturated (methyl stearate) through hydrogenation is a step that occurs in a short time. Similar results were obtained in some studies (Van Den Hark *et al.* 1999, Thakur and Kundu 2016) when hydrogenating unsaturated substrates. VAN and collaborators (Van Den Hark *et al.* 1999) stated that in the hydrogenation of FAME, the C-C double bonds undergo saturation first. This finding can support the fact that up to 5 min of reaction, regardless of the catalyst, did not exist among the esters carbon-carbon double bonds; there were only traces of esters with a double bond (methyl oleate). At the same time, fatty alcohol formation reactions occur. It can be observed the formation of wax esters, which are more stable intermediates in the process so that they can be considered as being transformed into fatty alcohols through the hydrogenation reaction, a determining step of the reaction (slower stage).

Conversion of palm esters: Based on the results presented in Figure 7, the conversion rate of palm esters is faster at temperatures of 280 ºC-70bar (Figure 7b) compared to the reactions carried out at 250 ºC-70bar (Figure 7a). The same conversion profile is observed for reactions performed at a pressure of 40 bar: at 280 ºC (Figure 7c) and 250 ºC (Figure 7d). Similar results have already been reported in the literature (Haidegger and Hodossy 1962, Rozmysłowicz *et al.* 2015). These and other researchers mentioned above have pointed out the most significant influence that temperature has on the process. A comparative analysis of the three catalysts at the applied temperatures that the Re/Nb_2O_5 catalyst presented a higher reaction rate in the batch reactor than the other two catalysts (Re/TiO_2 and Re/Al_2O_3). However, the greatest evidence that the catalyst supported on niobium has the fastest reaction rate is illustrated in the reaction at 250 ºC.

This is because, in reactions at 280 ºC, the Re/Al_2O_3 catalyst's conversion rates are closer to the conversion rate of the Re/Nb_2O_5 catalyst. After five (5h) of reaction, these two catalysts have practically the same conversion above 95 % until the end of the reaction. In this context, the conversion rate of palm esters is: $Re/Nb_2O_5 > Re/Al_2O_3 > Re/TiO_2$. This difference in catalytic activity in conversion can be related both to the metal-support interactions according to TPR results. The more difficult reduction is associated with a greater interaction of the rhenium particles with alumina and with niobium showed higher conversion rates. Meanwhile, for the titanium catalyst with easier reduction (lower temperatures), it had the lowest reaction rates. The reactions carried out at 40 bar pressure show low conversion compared to the reactions carried out at 70 bar, both for the reactions at 250ºC and 280ºC. Therefore, this result indicates that pressure is also an essential factor in the conversion of esters.

Products formation of palm esters hydrogenation reaction: Figure 8 and Figure 9 shows a product formation profile (fatty alcohols and hydrocarbons) similar to the three catalysts. The difference consists of the rate of formation depending on the variation of pressure and temperature. Reactions carried out at 280 ºC, Figure 8 [Graph (a), Graph (c)] regardless of pressure (70 or 40 bar) show a higher rate of formation of fatty alcohols when compared to reactions carried out at 250 ºC, Figure 9 [Graph (a), Graph (c)]. However, the low temperatures 250 ºC-70 bar, [Figure 9, Graph (a)] (Re/Nb_2O_5 and Re/Al_2O_3) favored the formation of more fatty alcohols about the temperature of 280 ºC for the same catalysts. At a temperature of 280 ºC, [Figure 8, Graph (a)] although they had a high rate of formation of fatty alcohols, they underwent dehydration and hydrogenation, forming more hydrocarbons (C_{15}, C_{16}, C_{17}, and C_{18}) [Figure 8, Graph (b)]. The Re/TiO_2 catalyst was efficient in the formation of fatty alcohols at a temperature of 280 ºC-70 bar since it presented a low conversion of these into hydrocarbons. The reactions performed at 40 bar showed low formation of fatty alcohols and a 70 bar ratio. However, all catalysts have a similar degree of fatty alcohol formation for reactions carried out at 280 ºC-40 bar and 250 ºC-40 bar. However, the highest formation of fatty alcohols is always at 280 ºC. As for the formation of hydrocarbons Figure 8 [Graph (b), Graph (d)], it was also evident that high temperatures (280 ºC) favored the production of hydrocarbons more due to the reactions of dehydration, decarboxylation, and decarbonylation, at both pressures (40 and 70bar). On the other hand, the results show that high pressure (70 bar) favored hydrocarbons' formation more through hydrogenation reactions. In all reactions, regardless of temperature and pressure, the catalysts that produced the most hydrocarbons are (Re/Nb_2O_5 and Re/Al_2O_3).

Influence of Temperature and Pressure on Conversion and Selectivity

Re/Nb_2O_5 catalyst: Figure 10 shows the conversion and selectivity of products using the catalyst supported on niobia; it is observed that the product formation increases simultaneously, depending on the selectivity, fatty alcohol, wax ester, and hydrocarbon more excellent selectivity towards fatty alcohols. The description of the reactions involved in the reaction mechanisms proposed in Table 1. Observing, in Figure 10, the selectivity curves of wax esters and hydrocarbons affect the decrease in the selectivity of fatty alcohols; that is, as shown in Table 1 of the reaction equations, it is noticed that the wax esters are formed by the reaction of fatty acid esters and fatty alcohols. On the other hand, one of the main stages of the formation of fatty alcohols is the dehydration of fatty alcohols; that is, when one compound is consumed, the other produced, and vice versa.

Re/Al_2O_3 catalyst: It is also noted that the temperature is one of the determining factors in the selectivity of the products, at low temperatures, 250 ºC "Graph (a), and Graph (c)" the selectivity of fatty alcohols is right. The fatty alcohol produced

was not suffered from greater dehydration and conversion to hydrocarbons. This fact was observed in "Graph (b), and Graph (d)" of the same Figure 9; that is, it is possible to observe that the decrease in the selectivity of fatty alcohols is inversely proportional to the selectivity in hydrocarbons. The temperature also affects the conversion rate; in 4 h of reaction, at 250 ºC, the conversion was reached 85 %, while at 280 ºC, the conversion was above 95 %. Figure 11, referring to the use of the Re/Al_2O_3 catalyst, the esters and product selectivity curves present a profile similar to that shown in Figure 10, which used the Re/Nb_2O_5 catalyst since there is the evolution of compounds simultaneously. Both catalysts showed good catalytic activity; however, the conversion rate was faster in catalyst supported on Nb_2O_5 than Al_2O_3. Another aspect to highlight is the wax esters production in reactions at 250 ºC-70bar.

The Re/Nb_2O_5 catalyst is began formed from 2h of reaction until 7h, despite being in selectivity below 10%. In contrast, with the Re/Al_2O_3 catalyst, traces of wax esters appear at the beginning of the reaction but are quickly consumed. At 280 ºC-70bar, the two catalysts showed greater selectivity in hydrocarbons, which increases the longer the reaction time. Similar as what was observed with temperature, pressure plays an essential role in converting and selecting products. Higher pressure obtained better yield both in the conversion of esters and in the selectivity of fatty alcohols. Low pressures (40 bar) in addition to low conversion, obtained low selectivity in fatty alcohols and increased selectivity in wax esters. This can indicate that pressure is fundamental in the conversion of the intermediate; that is, the higher the reaction pressure, the higher the conversion rate of wax esters to fatty alcohols. The reaction pressure evaluation for the Re/Al_2O_3 catalyst suggests a profile similar to that presented in the Re/Nb_2O_5 catalyst. High pressures favored a higher reaction rate, having obtained high ester conversions and greater selectivity in fatty alcohols than at pressures of 40 bar of hydrogen.

Re/TiO_2 catalyst: Figure 12 shows the results of selectivity and conversion using the Re/TiO_2 catalyst. It can be seen that the reaction carried out at 250 ºC-70bar presents a profile similar to that of the other reactions carried out at the same temperature, but with other catalysts. While the reaction performed at 280 ºC-70bar shows at the beginning (in 1 h) that there was only the production of fatty alcohols, but after that time, it is possible to see a series reaction mechanism, at the beginning of the reaction, since the fatty alcohols are formed first, up to a reaction time of 1 h. From this moment on, a simultaneous evolution of the compounds is perceived. In this case, the fatty alcohol formation curve is the inverse of the hydrocarbon curve, which suggests a dominance of alcohol dehydration following hydrocarbons formation.

However, the yield of fatty alcohols is higher for longer residence times; this scenario works for both low (Graph (a) at Figure 12) and high (Graph (b) at Figure 12) temperatures. Thus, presenting conversions of 71.8 and 93.8 %, and selectivity is 85.6 and 92.1 % for low and high temperatures. The formation of wax esters at a temperature of 280 ºC-70 bar with the Re/TiO_2 catalyst was not significant since the wax ester does not appear as a reaction product. In general, the three catalysts behave similarly concerning the influence of pressure on hydrogenation reactions. Reactions performed at 70 bar achieved better performance than reactions performed at 40 bar. Another aspect is that low pressures have been shown to favor wax esters (reaction intermediates) than in reactions at 70 bar. In any case, the pressure variation decreases a pig's selectivity in unwanted products (hydrocarbons).

DISCUSSION OF KINETIC TEST RESULTS

The highest yield was obtained with the Re/Nb_2O_5 and Re/Al_2O_3 catalysts, which had the fastest reaction rate than the Re/TiO_2 catalyst activity. The higher conversion rate of the two catalysts can be attributed to a stronger interaction of rhenium precursor with the supports, and they probably present greater metallic dispersion. Re/TiO_2 catalyst showed greater selectivity of fatty alcohols both at 250, and 280 ºC than the Re/Nb_2O_5 and Re/Al_2O_3 catalysts, mainly in the reactions carried out at 280 ºC, regardless of the reaction pressure (40 or 70 bar) (Rozmysłowicz *et al.* 2015, Oi, Choo et al. 2016). The difference in the activity promoted by the catalysts can be related mainly to the supports' nature and properties. For the case of the Re/Nb_2O_5 catalyst, its support for being an acid oxide presented strong Brönsted acid sites, which promoted a rapid dehydration reaction of alcohol and tended to follow the hydrocarbon route, mainly the hydrodeoxygenation, which explains the greater selectivity in even hydrocarbons (C_{16} and C_{18}). Similar results were obtained in the work of (Kumar *et al.* 2014). The Re/Al_2O_3 catalyst, because it is supported by a refractory oxide and has a higher volume of pores, justifies the higher rate of conversions of the substrates and selectivity of fatty alcohols then convert to hydrocarbons, mainly at a temperature of 280 ºC. According to Kent *et al.* (2014), refractory oxide-supported catalysts are usually characterized by decarboxylation, decarbonylation, and hydrodeoxygenation reactions, preferably decarboxylation and decarbonylation.

In general, the distribution of products and their selectivity were influenced by temperature and the type of catalyst used. Low temperatures show low conversion rates and selectivity towards fatty alcohols. The correlation between temperature, pressure, and residence time is that the residence time influences the process yield. The longer the residence time, the greater the substrate's gradual conversion and the formation of fatty alcohols. Actually, the most significant advantage of reactions at low temperatures is the reduced possibility of converting fatty alcohols into hydrocarbons. When hydrogenating fatty acid esters, C=C unsaturated bonds first undergo saturation before hydrogenating the functional groups (fatty acids, esters, fatty alcohols, and aldehydes). According to Van Den Hark *et al.* (1999), this saturation occurs at temperatures below 200 ºC. The increase in the reaction rate can serve as a stepping stone to reduce secondary products' formation since this will decrease the accumulation of products on the catalyst surface. This act can considerably improve the selectivity of fatty alcohols, as illustrated in graphs (b) in Figures 7, 8 and 9. These graphs indicate a high reaction rate for the production of fatty alcohols. However, after 5h of reaction, the conversion of fatty alcohols drastically changes, favoring hydrocarbons formation. This aspect was also observed by several studies, for example (Zhilong 2011, Rozmysłowicz *et al.* 2015).

Our results show that the Re/TiO_2 catalyst, despite the slow conversion rate when compared to the conversion of Re/Al_2O_3 and Re/Nb_2O_5 catalysts, the Re/TiO_2 catalyst had better selectivity in fatty alcohols at 280 ºC. Similar results have

been obtained in the literature (Toyao, Siddiki et al. 2017, Di *et al.* 2019, Lawal 2019). The catalytic performance of catalysts is analyzed in detail. The Re/Nb_2O_5 catalyst showed a higher conversion rate and selectivity of fatty alcohols, mainly in all reactions except the reaction of 280ºC at 70 bar, because there was the conversion of fatty alcohols into hydrocarbons, as previously presented. This result may be related to factors: greater metallic dispersion of Re/Nb, according to the XPS results, and because this catalyst is the only one that presented a greater amount of Bronsted acid sites, although it also has Lewis acids, as they presented IFTR results. According to the literature (Foo *et al.* 2014, Leal *et al.* 2019), using Ni/Nb_2O_5 catalysts found that the decrease in Bronsted acids is detrimental to alcohol dehydration performance.

According to Foo *et al.* (2014), Brønsted acidic sites are more active for alcohol dehydration than Lewis acidic sites, so greater dehydration and hydrogenation of fatty alcohols. Leal *et al.* (2019) used Ni/Nb_2O_5 catalyst with different levels. They observed that catalysts with a lower nickel content showed a greater amount of Bronsted sites, consequently greater conversion of cyclohexanol. In comparison, catalysts with a higher nickel content decreased conversion of cyclohexanol due to fewer Bronsted acid sites and more Lewis acid sites. Therefore, this result may indicate that the 4% Re in the catalyst contributes to a greater amount of Bronsted acid sites, favoring the dehydration of fatty alcohols to the Re/Nb_2O_5 catalyst. As for the Re/Al_2O_3 catalyst, which also performed well in converting esters and in the formation of fatty alcohols. Therefore, with a performance profile similar to that obtained with Re/Nb_2O_5 catalyst, some factors can be pointed out. This yield may be mainly related to the fact that Re/Al_2O_3 has a larger surface area and a greater pore volume than Re/Nb_2O_5 and Re/TiO_2 catalysts (Miyake *et al.* 2009). However, it presents low metallic dispersion and practically Lewis acidic sites. The greater performance of this can be attributed to the use of solvent, taking into account that this catalyst has a higher pore volume, as observed by the material textural properties. Therefore, even if it presented more Lewis acid sites in the IFTR results and less metal dispersion in the XPS results, the solvent (heptane) increases the solubility of hydrogen in the substrate and decreases the resistance to mass transport (van den Hark and Härröd 2001, Zhilong 2011, Rozmysłowicz *et al.* 2015).

Our results show that the Re/TiO_2 catalyst, despite a slow conversion rate compared to the conversion of Re/Al_2O_3 and Re/Nb_2O_5 catalysts, the Re/TiO_2 catalyst better selectivity in fatty alcohols at a temperature of 280ºC. Similar results have been obtained in the literature (Toyao *et al.* 2017, Di *et al.* 2019, Lawal 2019). The Re/TiO_2 catalyst performed well in the conversion, but with a somewhat slow conversion rate. However, it was excellent in the selectivity of fatty alcohols. It was the only catalyst that fatty alcohols did not undergo much dehydration or hydrogenation, thus reducing the formation of hydrocarbons. The good performance may be related to the metallic dispersion of rhenium on titania. But, the preservation of hydroxyl and reduction of decarbonylation and decarboxylation reactions may be due to the balanced amount between the Bronsted and Lewis acidic sites. In the study of the conversion of acetic acid into ethanol and methane, the Re/TiO_2 catalyst showed more efficiency in converting acetic and selective acid in the formation of ethanol, compared to the catalyst supported on alumina and silica (Lawal 2019). In a study Toyao *et al.* (2017), fatty alcohols' good selectivity was

also obtained using Re/TiO_2 catalysts. Di *et al.* (2019), the low conversion obtained using the Re/TiO_2 catalyst was attributed to the high state of rhenium oxidation in the catalysts, which is neither favorable dehydrogenation nor to hydrogenolysis of cyclohexane. , for catalysts supported by titania. Some authors believe that the Re/TiO2 catalyst's greater activity may be due to carbonyl species' adsorption through interaction with the Ti^{n+} cations (Lewis acid sites) or oxygen waves created in the reducible oxide after reduction at 200 °C. These sites can activate the carboxyl acid group for hydrogenation (He and Wang 2012, Lawal 2019).

Influence of temperature and hydrogen pressure: The temperature was a very important factor in conversion and selectivity. The increase in temperature from 250 to 280 °C played a fundamental role in the production of fatty alcohols; that is, the higher the system temperature, the greater the conversion achieved. However, on the other hand, the temperature influences the dehydration of fatty alcohol to hydrocarbons (unwanted products). The products obtained in all reactions were the same. The difference consists of selectivity and conversion, depending on the type of catalyst used. In general, the catalysts showed a statistically equal conversion when comparing the results in the best conditions (280 ºC and 70 bar) obtained in the three catalysts Re/Nb_2O_5, Re/Al_2O_3, and Re/TiO_2. The low temperature (250 ºC) shows excellent yield in fatty alcohols because, after 8h of reaction, the conversion of esters achieved, and the selectivity of fatty alcohols is very high. Due to low temperatures, the fatty alcohols produced did not undergo high dehydration. In this case, selectivity favors the formation of wax esters, which are the fact that they are very stable intermediates in the reaction since their hydrogenation is slow. The increase in residence time was fundamental to increase conversion and selectivity, consequently yielding the reaction temperature. However, Van Den Hark *et al.* (1999) found that it was possible to obtain the extract's conversion into fatty alcohols in shorter residence time and at lower temperatures. Another aspect of being highlighted is the formation of intermediates, wax esters. It was evident that the production of these depends on both the temperature and the type of catalyst. However, some studies have obtained the aldehydes as intermediates for the reaction (Van Den Hark, Härröd et al. 1999, Rozmysłowicz *et al.* 2015). However, some researchers have obtained similar intermediates, wax esters (Hattori *et al.* 2000, van den Hark and Härröd 2001, Brands *et al.* 2002, Thakur and Kundu 2016).

The correlation between high temperature (280 ºC) and longer residence times indicates a favorable conversion rate of esters. However, the severe temperature conditions, 280 ºC, and pressure, 70 bar, decreased the selectivity in fatty alcohols, increasing the hydrocarbon yield. Similar results have been reported elsewhere (Van Den Hark, Härröd et al. 1999, Rozmysłowicz *et al.* 2015, Thakur and Kundu 2016). The increase in hydrocarbons' selectivity in those reaction conditions may be due to the dehydration of fatty alcohols by temperature or by their hydrogenation by hydrogen pressure. Because of this, some works suggest the application of mild conditions of temperature and pressure. An example of the reactions carried out at a temperature of 250 ºC that converted fatty alcohols to hydrocarbons was minimal. In this context, the reactions carried out at temperatures of 250 ºC using the Re/Al_2O_3 and Re/Nb_2O_5 catalysts had better yield in the production of fatty alcohols since they presented greater

selectivity, although the same catalysts at 280 ºC have shown greater conversion, the selectivity of fatty alcohols decreased, favoring the formation of hydrocarbons. Hattori *et al.* (2000) in their study found that catalysts supported on alumina play a vital role in the durability of catalysts. Alumina, in addition to increasing the life of catalysts, alumina ensures good activity and selectivity. Contrary to the work by BASSM *et al.* (2016), the ReS/TiO$_2$ catalyst was obtained in the production of fatty alcohols than with the ReS/Al$_2$O$_3$ catalyst. The authors believe that the Re/TiO2 catalyst's greater activity was correlated with the Re dispersion and ReS$_2$ species formation. This may be obvious since, in this work, the Re/TiO$_2$ dispersion may be greater than that of Re/Al$_2$O$_3$, but the Re/Al$_2$O$_3$ catalyst showed good activity. Perhaps the greatest catalytic performance obtained in the work of BASSM *et al.* (2016) of Re/TiO$_2$ that the catalysts' sulfide may have also influenced re/Al2O3. The Re/TiO$_2$ catalyst, at both temperatures, 250 and 280 ºC, showed better selectivity. According to van den Hark and Härröd (2001), the process viability is determined by conversion and economic viability. However, it is also determined by the product's selectivity of interest to achieve the best possible yield. In this perspective, the formation of secondary products such as hydrocarbons, aldehydes, and wax esters must be reduced.

According to Rozmysłowicz *et al.* (2015), the use of TiO$_2$ as support gave good results up to 93 % selectivity in fatty alcohols, at 180-220 ºC, and 20-40 bar due to the greater interaction between support and metal. The authors believe that the yield obtained was due to TiO$_2$ as a support because it is a reducible oxide allowing greater interaction between the catalyst components. The shorter the residence time at lower temperatures, the lower the substrate conversion and wax esters' higher selectivity. Van Den Hark *et al.* (1999) obtained similar results, where at low temperatures, they observed the highest selectivity in aldehydes (intermediates). On the other hand, to improve the yield of fatty alcohols, hydrogen pressure and low temperatures have been applied using an organic solvent to improve the extract's selectivity and solubility (ester or fatty acid) since the hydrogen is anti-solvent in the substrate (van den Hark and Härröd 2001). In monophasic reactions, the substrate has been a limiting factor due to difficulties maintaining the invariant conditions. Also, due to hydrogen's action, this is anti-solvent in the reaction, which reduces the solubility of the substrate and product in the reaction medium. However, to maintain homogeneous conditions and ensure good selectivity and conversion, the hydrogen pressure must be low.

Frequently in processes where there are low conversion and selectivity of fatty alcohols, there is a higher production of wax esters or aldehydes. Usually, these intermediates' formation is fast, but their conversion into fatty alcohols or hydrocarbons is not very flexible under certain operating conditions. Van den Hark and Härröd (2001) found a total conversion of esters and intermediates' formation. However, the reaction continues to take longer for these to be converted into the final product. In general, the highest conversions of esters and alcohol yields were achieved in reactions with 70 bar pressures compared to 40 bar pressures, regardless of the reaction temperature. That is means that the higher the system pressure, the greater the conversion of esters and the more excellent selectivity of fatty alcohols. Similar results have been reported in the literature (Toba *et al.* 1999, Rozmysłowicz *et al.* 2015). Reactions performed at a 40 bar pressure were

selective in forming the intermediate (wax esters). However, high pressures increase the hydrogenation rate of these in fatty alcohols, as already been demonstrated in the literature (van de Scheur and Staal 1994, Huang *et al.* 2009).

Conclusion

The results show that the catalysts presented a good performance regarding the conversion of palm esters and product selectivity to fatty alcohols. It was evident that temperature and residence time are fundamental parameters for product conversion and selectivity. The higher the temperature, the higher the conversion rate of esters. But lower was the fatty alcohol yield due to dehydration throughout the reaction, except for Re/TiO$_2$ catalyst. The increase in residence time was fundamental to increase conversion selectivity and, consequently, the yield, regardless of the reaction temperature. Different support types were essential to evaluate their catalytic activity; therefore, the Re/Al$_2$O$_3$ and Re/Nb$_2$O$_5$ catalysts showed a higher reaction rate but less selectivity in fatty alcohols in longer periods due to preferential reactions to dehydration, decarboxylation, and decarbonylation. While Re/TiO$_2$ catalyst, despite the low reaction rate, showed greater selectivity to fatty alcohols. The results show that the Re/Nb$_2$O$_5$ catalyst showed excellent catalytic activity at 250 ºC and 70 bar. The metallic dispersion, types of acidic sites, the interaction between rhenium with the different supports, pore-volume, surface area, and the solvent (heptane) were decisive to explain the difference in the catalytic performance of the catalysts. Greater selectivity in the Re/TiO$_2$ catalyst's fatty alcohols at 280ºC-70bar than the Re/Nb$_2$O$_5$ and Re/Al$_2$O$_3$ catalysts may have been because the Re/TiO$_2$ catalyst has a balanced amount of Bronsted and Lewis acid sites, and probably because TiO$_2$ is a reducible oxide.

REFERENCES

Agarwal, P., S. S. Al-Khattaf and M. T. Klein 2019. "Molecular-Level Kinetic Modeling of Triglyceride Hydroprocessing." Energy & Fuels 338: 7377-7384.

Agarwal, P., N. Evenepoel, S. S. Al-Khattaf and M. T. Klein 2018. "Molecular-level kinetic modeling of methyl laurate: The intrinsic kinetics of triglyceride hydroprocessing." Energy & Fuels 324: 5264-5270.

Ali, A., B. Li, Y. Lu and C. Zhao 2019. "Highly selective and low-temperature hydrothermal conversion of natural oils to fatty alcohols." Green Chemistry 2111: 3059-3064.

Augustine, S. M. and W. M. Sachtler 1989. "On the mechanism for the platinum-catalyzed reduction of rhenium in PtReγ-Al2O3." Journal of Catalysis 1161: 184-194.

Azzam, K., I. Babich, K. Seshan and L. Lefferts 2007. "A bifunctional catalyst for the single-stage water–gas shift reaction in fuel cell applications. Part 2. Roles of the support and promoter on catalyst activity and stability." Journal of catalysis 2511: 163-171.

Bare, S. R., S. D. Kelly, F. D. Vila, E. Boldingh, E. Karapetrova, J. Kas, G. E. Mickelson, F. S. Modica, N.

Yang and J. J. Rehr 2011. "Experimental XAS, STEM, TPR, and XPS and theoretical DFT characterization of supported rhenium catalysts." The Journal of Physical Chemistry C 11513: 5740-5755.

BASSM, R., M. Villarroel, F. Gil-Llambias, P. Baeza, J. García-Fierro, N. Martínez, P. Olivera, K. Leiva and N. Escalona 2016. "SUPPORT EFFECT ON CONVERSION OF QUINOLINE OVER ReS2 CATALYST." Journal of the Chilean Chemical Society 614: 3170-3176.

Benítez, C. A. F., V. A. Mazzieri, M. A. Sánchez, V. M. Benitez and C. L. Pieck 2019. "Selective hydrogenation of oleic acid to fatty alcohols on Rh-Sn-B/Al2O3 catalysts. Influence of Sn content." Applied Catalysis A: General 584: 117149.

Boelhouwer, C., J. Snelderwaard and H. Waterman 1956. "Problems of selectivity in the hydrogenation of linoleic acid esters." Journal of the American Oil Chemists Society 334: 143-146.

Brands, D., K. Pontzen, E. Poels, A. Dimian and A. Bliek 2002. "Solvent□based fatty alcohol synthesis using supercritical butane: Flowsheet analysis and process design." Journal of the American Oil Chemists' Society 791: 85-91.

Burch, R., C. Paun, X.-M. Cao, P. Crawford, P. Goodrich, C. Hardacre, P. Hu, L. McLaughlin, J. Sa and J. Thompson 2011. "Catalytic hydrogenation of tertiary amides at low temperatures and pressures using bimetallic Pt/Re-based catalysts." Journal of catalysis 2831: 89-97.

Carnahan, J., T. Ford, W. Gresham, W. Grigsby and G. Hager 1955. "Ruthenium-catalyzed hydrogenation of acids to alcohols." Journal of the American Chemical Society 7714: 3766-3768.

Chia, M., B. J. O'Neill, R. Alamillo, P. J. Dietrich, F. H. Ribeiro, J. T. Miller and J. A. Dumesic 2013. "Bimetallic RhRe/C catalysts for the production of biomass-derived chemicals." Journal of catalysis 308: 226-236.

Cui, X., Y. Li, C. Topf, K. Junge and M. Beller 2015. "Direct Ruthenium□Catalyzed Hydrogenation of Carboxylic Acids to Alcohols." Angewandte Chemie 12736: 10742-10745.

da SQ Menezes, J. P., K. R. Duarte, R. L. Manfro and M. M. Souza 2020. "Effect of niobia addition on cobalt catalysts supported on alumina for glycerol steam reforming." Renewable Energy 148: 864-875.

Di, X., G. Lafaye, C. Especel, F. Epron, J. Qi, C. Li and C. Liang 2019. "Supported Co–Re Bimetallic Catalysts with Different Structures as Efficient Catalysts for Hydrogenation of Citral." ChemSusChem 124: 807-823.

Escalona, N., J. Ojeda, J. Palacios, M. Yates, J. Fierro, A. L. Agudo and F. Gil-Llambías 2007. "Promotion of Re/Al2O3 and Re/C catalysts by Ni sulfide in the HDS and HDN of gas oil: Effects of Ni loading and support." Applied Catalysis A: General 319: 218-229.

Foo, G. S., D. Wei, D. S. Sholl and C. Sievers 2014. "Role of Lewis and Brønsted acid sites in the dehydration of glycerol over niobia." Acs Catalysis 49: 3180-3192.

Ghampson, I. T., C. Sepúlveda, R. García, J. L. Fierro and N. Escalona 2016. "Carbon nanofiber-supported ReO x catalysts for the hydrodeoxygenation of lignin-derived compounds." Catalysis Science & Technology 612: 4356-4369.

Grau, R. J., A. E. Cassano and M. A. Baltanás 1988. "Catalysts and network modeling in vegetable oil hydrogenation processes." Catalysis Reviews Science and Engineering 301: 1-48.

Griffith, K. J., A. C. Forse, J. M. Griffin and C. P. Grey 2016. "High-rate intercalation without nanostructuring in metastable Nb2O5 bronze phases." Journal Pd the American Chemical Society 13828: 8888-8899.

Hachemi, I. and D. Y. Murzin 2018. "Kinetic modeling of fatty acid methyl esters and triglycerides hydrodeoxygenation over nickel and palladium catalysts." Chemical Engineering Journal 334: 2201-2207.

Haidegger, E. and L. Hodossy 1962. "Technologische Bedingungen zur Herstellung von Fettalkoholen durch katalytische Hochdruck□Hydrierung." Fette, Seifen, Anstrichmittel 644: 326-329.

Hattori, Y., K. Yamamoto, J. Kaita, M. Matsuda and S. Yamada 2000. "The development of nonchromium catalyst for fatty alcohol production." Journal of the American Oil Chemists' Society 7712: 1283-1288.

He, Z. and X. Wang 2012. "Hydrodeoxygenation of model compounds and catalytic systems for pyrolysis bio-oils upgrading." Catalysis for sustainable energy 11: 28-52.

Hilmen, A., D. Schanke and A. Holmen 1996. "TPR study of the mechanism of rhenium promotion of alumina-supported cobalt Fischer-Tropsch catalysts." Catalysis letters 383-4: 143-147.

Huang, H., G. Cao, C. Fan, S. Wang and S. Wang 2009. "Effect of water on Cu/Zn catalyst for hydrogenation of fatty methyl ester to fatty alcohol." Korean journal of chemical engineering 266: 1574-1579.

Isaacs, B. H. and E. E. Petersen 1982. "The effect of drying temperature on the temperature-programmed reduction profile of a platinum/rhenium/alumina catalyst." Journal of Catalysis 771: 43-52.

Kent, P. D., J. E. Mondloch and R. G. Finke 2014. "A Four-Step Mechanism for the Formation of Supported-Nanoparticle Heterogenous Catalysts in Contact with Solution: The Conversion of Ir 1, 5-COD Cl/γ-Al2O3 to Ir 0□ 170/γ-Al2O3." Journal of the American Chemical Society 1365: 1930-1941.

Kerkhof, F. and J. Moulijn 1979. "Quantitative analysis of XPS intensities for supported catalysts." Journal of Physical Chemistry 8312: 1612-1619.

Kirilin, A. 2013. Aqueous-phase reforming of renewables for selective hydrogen production in the presence of supported platinum catalysts, Aqueous-phase reforming of renewables for selective hydrogen production in the presence of supported platinum catalysts, Åbo Akademi University.

Kumar, P., S. R. Yenumala, S. K. Maity and D. Shee 2014. "Kinetics of hydrodeoxygenation of stearic acid using supported nickel catalysts: Effects of supports." Applied Catalysis A: General 471: 28-38.

Lawal, A. M. 2019. Catalytic upgrading of bio-oil via the hydrodeoxygenation of short chain carboxylic acids, Catalytic upgrading of bio-oil via the hydrodeoxygenation of short chain carboxylic acids, University of Birmingham.

Leal, G. F., S. Lima, I. Graça, H. Carrer, D. H. Barrett, E. Teixeira-Neto, A. A. S. Curvelo, C. B. Rodella and R. Rinaldi 2019. "Design of nickel supported on water-tolerant Nb2O5 catalysts for the hydrotreating of lignin streams obtained from lignin-first biorefining." Iscience 15: 467-488.

Ly, B. K., B. Tapin, M. Aouine, P. Delichere, F. Epron, C. Pinel, C. Especel and M. Besson 2015. "Insights into the oxidation state and location of rhenium in Re□Pd/TiO2 catalysts for aqueous□phase selective hydrogenation of succinic acid to 1, 4□butanediol as a function of palladium

and rhenium deposition methods." ChemCatChem 714: 2161-2178.

Ma, L., L. Yan, A.-H. Lu and Y. Ding 2018. "Effect of Re promoter on the structure and catalytic performance of Ni–Re/Al 2 O 3 catalysts for the reductive amination of monoethanolamine." RSC advances 815: 8152-8163.

Madsen, A. T., C. H. Christensen, R. Fehrmann and A. Riisager 2011. "Hydrodeoxygenation of waste fat for diesel production: Study on model feed with Pt/alumina catalyst." Fuel 9011: 3433-3438.

Malinowski, A., W. Juszczyk, M. Bonarowska, J. Pielaszek and Z. Karpiński 1998. "Pd-Re/Al2O3: Characterization and catalytic activity in hydrodechlorination of CCl2F2." Journal of Catalysis 1772: 153-163.

Manyar, H. G., C. Paun, R. Pilus, D. W. Rooney, J. M. Thompson and C. Hardacre 2010. "Highly selective and efficient hydrogenation of carboxylic acids to alcohols using titania supported Pt catalysts." Chemical communications 4634: 6279-6281.

Massa, M., A. Andersson, E. Finocchio and G. Busca 2013. "Gas-phase dehydration of glycerol to acrolein over Al2O3-, SiO2-, and TiO2-supported Nb-and W-oxide catalysts." Journal of Catalysis 307: 170-184.

Masuda, T., T. Takahashi and T. Higashimura 1985. "Polymerization of 1-phenyl-1-alkynes by halides of niobium and tantalum." Macromolecules 183: 311-317.

Mendes, M., O. Santos, E. Jordao and A. Silva 2001. "Hydrogenation of oleic acid over ruthenium catalysts." Applied Catalysis A: General 2171-2: 253-262.

Miyake, T., T. Makino, S.-i. Taniguchi, H. Watanuki, T. Niki, S. Shimizu, Y. Kojima and M. Sano 2009. "Alcohol synthesis by hydrogenation of fatty acid methyl esters on supported Ru–Sn and Rh–Sn catalysts." Applied Catalysis A: General 3641-2: 108-112.

Naglic, M., A. Smidovnik and T. Koloini 1998. "Kinetics of catalytic transfer hydrogenation of some vegetable oils." Journal of the American Oil Chemists' Society 755: 629-634.

Ni, J., W. Leng, J. Mao, J. Wang, J. Lin, D. Jiang and X. Li 2019. "Tuning electron density of metal nickel by support defects in Ni/ZrO2 for selective hydrogenation of fatty acids to alkanes and alcohols." Applied Catalysis B: Environmental 253: 170-178.

Ohama, Y. and D. Van Gemert 2011. Application of titanium dioxide photocatalysis to construction materials: state-of-the-art report of the RILEM Technical Committee 194-TDP, Springer Science & Business Media.

Oi, L. E., M.-Y. Choo, H. V. Lee, H. C. Ong, S. B. Abd Hamid and J. C. Juan 2016. "Recent advances of titanium dioxide TiO 2 for green organic synthesis." Rsc Advances 6110: 108741-108754.

Okal, J. 2005. "A study of effect of particle size on the oxidation of rhenium in the Re/γ-Al2O3 catalysts." Applied Catalysis A: General 2872: 214-220.

Okal, J., W. Tylus and L. Kępiński 2004. "XPS study of oxidation of rhenium metal on γ-Al2O3 support." Journal of Catalysis 2252: 498-509.

Paulis, M., M. Martın, D. Soria, A. Dıaz, J. Odriozola and M. Montes 1999. "Preparation and characterization of niobium oxide for the catalytic aldol condensation of acetone." Applied Catalysis A: General 1801-2: 411-420.

Ros, S. d., M. Schwaab and J. C. Pinto 2017. "Parameter estimation and statistical methods." Reedijk, Jan Ed.. Reference module in chemistry, molecular sciences and chemical engineering [recurso eletrônico].[Amsterdam: Elsevier, 2017]. 21 p.

Rozmysłowicz, B., A. Kirilin, A. Aho, H. Manyar, C. Hardacre, J. Wärnå, T. Salmi and D. Y. Murzin 2015. "Selective hydrogenation of fatty acids to alcohols over highly dispersed ReOx/TiO2 catalyst." Journal of Catalysis 328: 197-207.

Schäfer, H., R. Gruehn and F. Schulte 1966. "The modifications of niobium pentoxide." Angewandte Chemie International Edition in English 51: 40-52.

Scholfield, C., J. Nowakowska and H. Dutton 1962. "Hydrogenation of linolenate. IV. Kinetics of catalytic and homogeneous chemical reduction." Journal of the American Oil Chemists' Society 392: 90-95.

Schwaab, M. and J. C. Pinto 2007. "Optimum reference temperature for reparameterization of the Arrhenius equation. Part 1: Problems involving one kinetic constant." Chemical Engineering Science 6210: 2750-2764.

Shao, Y., Q. Xia, L. Dong, X. Liu, X. Han, S. F. Parker, Y. Cheng, L. L. Daemen, A. J. Ramirez-Cuesta and S. Yang 2017. "Selective production of arenes via direct lignin upgrading over a niobium-based catalyst." Nature communications 81: 1-9.

Somorjai, G. A. and Y. Li 2010. Introduction to surface chemistry and catalysis, John Wiley & Sons.

Thakur, D. S. and A. Kundu 2016. "Catalysts for fatty alcohol production from renewable resources." Journal of the American Oil Chemists' Society 9312: 1575-1593.

Thompson, S. T. and H. H. Lamb 2016. "Palladium–Rhenium Catalysts for Selective Hydrogenation of Furfural: Evidence for an Optimum Surface Composition." ACS Catalysis 611: 7438-7447.

Ting, K. W., T. Toyao, S. H. Siddiki and K.-i. Shimizu 2019. "Low-temperature hydrogenation of CO2 to methanol over heterogeneous TiO2-Supported Re catalysts." ACS Catalysis 94: 3685-3693.

Toba, M., S.-i. Tanaka, S.-i. Niwa, F. Mizukami, Z. Koppány, L. Guczi, K.-Y. Cheah and T.-S. Tang 1999. "Synthesis of alcohols and diols by hydrogenation of carboxylic acids and esters over Ru–Sn–Al2O3 catalysts." Applied Catalysis A: General 1892: 243-250.

Toyao, T., S. Siddiki, A. S. Touchy, W. Onodera, K. Kon, Y. Morita, T. Kamachi, K. Yoshizawa and K.-i. Shimizu 2017. "TiO2-Supported Re as a general and chemoselective heterogeneous catalyst for hydrogenation of carboxylic acids to alcohols." Chemistry-A European journal 235: 1001-1006.

Toyao, T., S. H. Siddiki, Y. Morita, T. Kamachi, A. S. Touchy, W. Onodera, K. Kon, S. Furukawa, H. Ariga and K. Asakura 2017. "Rhenium-Loaded TiO2: A Highly Versatile and Chemoselective Catalyst for the Hydrogenation of Carboxylic Acid Derivatives and the N-Methylation of Amines Using H-2 and CO2." Chemistry-A European journal 2359: 14848-14859.

van de Scheur, F. T. and L. H. Staal 1994. "Effects of zinc addition to silica supported copper catalysts for the hydrogenolysis of esters." Applied Catalysis A: General 1081: 63-83.

van den Hark, S. and M. Härröd 2001. "Fixed-bed hydrogenation at supercritical conditions to form fatty alcohols: the dramatic effects caused by phase transitions in the reactor." Industrial & engineering chemistry research 4023: 5052-5057.

Van Den Hark, S., M. Härröd and P. Møller 1999. "Hydrogenation of fatty acid methyl esters to fatty alcohols

at supercritical conditions." Journal of the American Oil Chemists' Society 7611: 1363-1370.

Viet, A. L., M. Reddy, R. Jose, B. Chowdari and S. Ramakrishna 2010. "Nanostructured Nb2O5 polymorphs by electrospinning for rechargeable lithium batteries." The Journal of Physical Chemistry C 1141: 664-671.

Yenumala, S. R., S. K. Maity and D. Shee 2017. "Reaction mechanism and kinetic modeling for the hydrodeoxygenation of triglycerides over alumina supported nickel catalyst." Reaction Kinetics, Mechanisms and Catalysis 1201: 109-128.

Yide, X., W. Xinguang, S. Yingzhen, Z. Yihua and G. Xiexian 1986. "Effect of various pretreatments on rhenium oxide-alumina catalysts: the structure and activity of active sites for propene metathesis." Journal of Molecular Catalysis 361-2: 79-89.

Zhang, L., A. M. Karim, M. H. Engelhard, Z. Wei, D. L. King and Y. Wang 2012. "Correlation of Pt–Re surface properties with reaction pathways for the aqueous-phase reforming of glycerol." Journal of Catalysis 287: 37-43.

Zhao, Y., X. Zhou, L. Ye and S. Chi Edman Tsang 2012. "Nanostructured Nb2O5 catalysts." Nano Reviews 31: 17631.

Zhilong, Y. 2011. Research on Hydrogenation of FAME to Fatty Alcohols at Supercritical Conditions. BIODIESEL– QUALITY, EMISSIONS AND BY-PRODUCTS, InTech: 171.

Zhou, C., Y. Zhao, T. Bian, L. Shang, H. Yu, L.-Z. Wu, C.-H. Tung and T. Zhang 2013. "Bubble template synthesis of Sn 2 Nb 2 O 7 hollow spheres for enhanced visible-light-driven photocatalytic hydrogen production." Chemical Communications 4984: 9872-9874.

Zhou, L., W. Lin, K. Liu, Z. Wang, Q. Liu, H. Cheng, C. Zhang, M. Arai and F. Zhao 2020. "Hydrodeoxygenation of ethyl stearate over Re-promoted Ru/TiO 2 catalysts: rate enhancement and selectivity control by the addition of Re." Catalysis Science & Technology 101: 222-230.

****